Development of an Interval Type-2 Fuzzy PID Controller based on Nie–Tan Defuzzification

Khushboo Kumari[1] B.M. Mohan[2] and Kiran Kumari[1]

***Abstract*—Interval Type-2 (IT2) Fuzzy Logic Controllers (FLCs) are widely used due to their superior control performance compared to their Type-1 (T1) equivalents. The Fuzzy PID (FPID) controller incorporating Non-Uniformly Distributed (NUD) Fuzzy Sets (FSs) outperforms the simplest FPID controller in handling complex dynamical systems. Therefore, this paper presents the analytical structures of a general IT2 FPID controller of Mamdani-type by considering NUD triangular-shaped IT2 FSs for input/output variables. Nie-Tan (NT) defuzzification and Larsen Product (LP) inference are employed to derive the mathematical models of the newly developed controller. To reduce the computational complexity, a one-dimensional (1D) input space is employed. The analytical structures of the developed controller are extensively examined for their properties. The robustness property of the developed controller is illustrated by considering output disturbance and plant parameter uncertainty during simulation studies.**

***Index Terms*—IT2 fuzzy PID control, Non-uniformly distributed fuzzy sets, Larsen product inference, Nie-Tan defuzzification.**

I. Introduction

Du and Ying [3] derived the mathematical structures of IT2 Fuzzy PI (FPI) and Fuzzy PD (FPD) controllers employing a Centroid defuzzifier and Average defuzzifier. Nie and Tan [4] obtained the structures of IT2 FPI/FPD controllers utilizing the Zadeh AND operator and the Karnik-Mendel (KM) Type Reduction (TR). Numerous models of T1 FPID controllers using 1D, 2D, and 3D input spaces are presented in the literature. However, very few models of IT2 FPID controllers are available. EI-Nagar and EI-Bardini [6] developed mathematical models of a 1D IT2 FPID controller. Kumar and Kumar [7] proposed an IT2 Fractional Order (FO) FPID controller. Sain et al. [9] derived mathematical models for both integer-order and FO 1D IT2 FPID controllers. Then, Praharaj et al. [10] extended this work to general 1D IT2 FPID controllers by considering NUD multiple IT2 FSs. A complete model was developed by Wang et al. [11] to represent the combined effects of defective measurements and randomly perturbed sampling periods by using stochastic variable sequences and Markov processes. Sain and Lee [12] derived few models of TS IT2 FPID controllers with the use of bottom-wide and top-wide triangular footprints of uncertainty (FoU). Various research works were devoted to the applications of fuzzy control. It is evident from the literature that IT2 FLCs are widely used controllers these days due to their ability to deal with high levels of uncertainty/disturbance in various real-world applications. Although many researchers have studied IT2 FLCs, there are still some unresolved issues, such as the defuzzification methods for modeling IT2 FPID controllers. The majority of defuzzification methods reported in the literature so far are approximate in their nature, and some are iterative. For the modeling of IT2 FPID, these defuzzification methods are too complex. Therefore, for ease of calculation, a 1D input space is used with the NT defuzzification technique.

It is observed from the literature that controllers with NUD input and output FSs provide better responses as compared to the controllers having Uniformly Distributed (UD) FSs [2] for an effective control design. Moreover, Praharaj et al. [10] proposed an IT2 FPID controller by considering NUD singletons as the output FSs. It is very much true that obtaining the IT2 FPID controller's models is difficult. The situation becomes more complicated if we use NUD triangular-shaped IT2 FSs to fuzzify input/output variables. Therefore, the objective of this paper is to derive models for general IT2 FPID controllers where NUD triangular-shaped IT2 FSs are used for fuzzifying both input and output variables. This research is crucial for handling nonlinear system control in an efficient manner, because in the control of nonlinear systems, both nonlinearities and the dynamics of the system need to be compensated simultaneously. Nonlinearity compensation depends on both the number and arrangement of FSs. These observations motivated us to study such an important problem.

Main contributions: To simplify the complexities in modeling of the IT2 FPID controller, a 1D input space has been used, in which the Fuzzy Proportional (FP), Fuzzy Integral (FI), and Fuzzy Derivative (FD) elements are realized separately and then integrated to generate the PID action. In this approach, fuzzy AND and OR operators are not required. NUD triangular-shaped IT2 FSs are considered for fuzzifying the variables for both input and output. The authors obtain the models of the controller using the NT defuzzification method.

II. Mathematical Preliminaries

The developed IT2 FPID controller's setup is shown in [9]. A typical linear PID controller's expression is provided as

$$u_{PID}(t) = K_P^c e(t) + K_I^c \int_0^t e(\tau)d\tau + K_D^c \dot{e}(t) \tag{1}$$

*This work was supported by the Council of Scientific and Industrial Research (CSIR), India.

[1]Khushboo Kumari and [1]Kiran Kumari are with the Department of Electrical Engineering, Indian Institute of Science, Bengaluru, India. [2] B. M. Mohan with the Department of Electrical Engineering, Indian Institute of Technology Kharagpur, West Midnapore, India. khushboo.prasad248@gmail.com; mohan@ee.iitkgp.ac.in; kirank@iisc.ac.in

Upon differentiation and discretization [9], we have

$$\Delta u_{PID}(k) = K_P^c \Delta e(k) + T K_I^c e(k) + \frac{K_D^c}{T} \Delta^2 e(k) \quad (2)$$

$$= K_P^d \Delta e(k) + K_I^d e(k) + K_D^d \Delta^2 e(k) \quad (3)$$

$$= \Delta e_s(k) + e_s(k) + \Delta^2 e_s(k) \quad (4)$$

where $\Delta u_{PID}(k) = u_{PID}(k) - u_{PID}(k-1)$, $K_P^d = K_P^c$, $K_I^d = T K_I^c$, and $K_D^d = \frac{K_D^c}{T}$ are the gains of the linear discrete-time controller. The IT2 FPID controller's $\Delta u_{PID}(k)$ is provided by

$$\Delta u_{PID}(k) = \gamma_p(\Delta e_s)\Delta e_s(k) + \gamma_I(e_s)e_s(k) + \gamma_D(\Delta^2 e_s)\Delta^2 e_s(k)$$
$$= \Delta u_P(k) + \Delta u_I(k) + \Delta u_D(k) \quad (5)$$

The gains related to the IT2 FP/FI/FD controllers are $\gamma_p(\Delta e_s)$/$\gamma_I(e_s)$/$\gamma_D(\Delta^2 e_s)$. The outcomes provided by the IT2 FP, IT2 FI, and IT2 FD controllers can be algebraically added to determine the outcome of the IT2 FPID controller, as demonstrated by (5). From here on, argument k is omitted for writing convenience. The description of the notations used in the above equations is given in Table I.

TABLE I: Notation description

Notation	Meaning	
K_P^c/K_P^d	Proportional gain of continuous/digital controller	
K_I^c/K_I^d	Integral gain of continuous/digital controller	
K_D^c/K_D^d	Derivative gain of continuous/digital controller	
$\Delta u_{P/I/D}(k)$	Change in control effort of P/I/D controller	
$\Delta u_{PID}(k)$	Change in control effort of PID controller	
$e_s(k)$	Scaled error	$e_s(k) = K_I^d e(k)$
$\Delta e_s(k)$	Scaled change in error	$\Delta e_s(k) = K_P^d \Delta e(k)$
$\Delta^2 e_s(k)$	Scaled double change in error,	$\Delta^2 e_s(k) = K_D^d \Delta^2 e(k)$

A. Fuzzification

Fuzzification maps a crisp value into an IT2 FS for each point of the Universe of Discourse (UoD). Figures 1 and 2 represent the IT2 FSs of input and output variables, respectively, along with their Membership Functions (MFs). The description of symbols is presented in Table II. Praharaj et al. [10] observed that for the trapezoidal type FoU, when the FoU covers both sides of the T1 MF, the controller becomes unsuitable for control, whereas when the upper MF matches with the T1 MF, the controller becomes suitable for control purposes. Therefore, in this study, we consider the case when the upper MF matches the T1 MF. The mathematical description of the i^{th} and $(i+1)^{th}$ FSs on input x is defined as follows:

$$\mu_{X_{i_l}} = \begin{cases} \frac{-x+L_{x_{i+1}}-P_{x_i}}{L_{x_{i+1}}-L_{x_i}} & \text{if } L_{x_i} \le x \le (L_{x_{i+1}} - P_{x_i}) \\ 0 & \text{if } (L_{x_{i+1}} - P_{x_i}) \le x \le L_{x_{i+1}} \end{cases} \quad (6)$$

$$\mu_{X_{i_u}} = \left\{ \frac{-x+L_{x_{i+1}}}{L_{x_{i+1}}-L_{x_i}} \quad \text{if } L_{x_i} \le x \le L_{x_{i+1}} \right. \quad (7)$$

$$\mu_{X_{(i+1)_l}} = \begin{cases} 0 & \text{if } L_{x_i} \le x \le (L_{x_i} + P_{x_i}) \\ \frac{x-L_{x_i}-P_{x_i}}{L_{x_{i+1}}-L_{x_i}} & \text{if } (L_{x_i} + P_{x_i}) \le x \le L_{x_{i+1}} \end{cases} \quad (8)$$

$$\mu_{X_{(i+1)_u}} = \left\{ \frac{x-L_{x_i}}{L_{x_{i+1}}-L_{x_i}} \quad \text{if } L_{x_i} \le x \le L_{x_{i+1}} \right. \quad (9)$$

where $\mu_{X_{i_l}}$ and $\mu_{X_{i_u}}$ are the lower and upper MFs of i^{th} input FS, and $\mu_{X_{(i+1)_l}}$ and $\mu_{X_{(i+1)_u}}$ are the lower and upper MFs of $(i+1)^{th}$ input FS.

TABLE II: Symbols description

Symbol	FP controller	FI controller	FD controller
c	P	I	D
x	Δe_s	e_s	$\Delta^2 e_s$
y	Δu_P	Δu_I	Δu_D
X_{i_l}	ΔE_{i_l}	E_{i_l}	$\Delta^2 E_{i_l}$
X_{i_u}	ΔE_{i_u}	E_{i_u}	$\Delta^2 E_{i_u}$
$X_{(i+1)_l}$	$\Delta E_{(i+1)_l}$	$E_{(i+1)_l}$	$\Delta^2 E_{(i+1)_l}$
$X_{(i+1)_u}$	$\Delta E_{(i+1)_u}$	$E_{(i+1)_u}$	$\Delta^2 E_{(i+1)_u}$
Y_{i_l}	ΔU_{Pi_l}	ΔU_{Ii_l}	ΔU_{Di_l}
Y_{i_u}	ΔU_{Pi_u}	ΔU_{Ii_u}	ΔU_{Di_u}
$Y_{(i+1)_l}$	$\Delta U_{P(i+1)_l}$	$\Delta U_{I(i+1)_l}$	$\Delta U_{D(i+1)_l}$
$Y_{(i+1)_u}$	$\Delta U_{P(i+1)_u}$	$\Delta U_{I(i+1)_u}$	$\Delta U_{D(i+1)_u}$

We assume in Figs. 1 and 2 that the FSs are NUD, that is

$$L_{x_{i+2}} - L_{x_{i+1}} \neq L_{x_{i+1}} - L_{x_i} \neq L_{x_i} - L_{x_{i-1}} \quad \text{(in Fig. 1)}$$
$$L_{y_{i+2}} - L_{y_{i+1}} \neq L_{y_{i+1}} - L_{y_i} \neq L_{y_i} - L_{y_{i-1}} \quad \text{(in Fig. 2)}$$

and J_x and J_y are the numbers of FSs considered for fuzzifying the input and output variables, respectively. The degree of uncertainty in membership value is defined by θ_x (or θ_y) in Fig. 1 (or 2). Keep in mind that θ_x, $\theta_y \in [0, 0.5]$. It is possible to determine, using basic geometry, that

$$P_{x_{i-1}} = (L_{x_i} - L_{x_{i-1}})\theta_x, P_{x_i} = (L_{x_{i+1}} - L_{x_i})\theta_x$$
$$P_{x_{i+1}} = (L_{x_{i+2}} - L_{x_{i+1}})\theta_x, P_{y_{i-1}} = (L_{y_i} - L_{y_{i-1}})\theta_y$$
$$P_{y_i} = (L_{y_{i+1}} - L_{y_i})\theta_y, P_{y_{i+1}} = (L_{y_{i+2}} - L_{y_{i+1}})\theta_y$$

B. Control rule base

The NUD IT2 FP/IT2 FI/IT2 FD controller has the following rules:

$R_{1c} : [R_{1lc}, R_{1uc}]$: IF x is $[X_{i_l}, X_{i_u}]$ THEN Δu_c is $[Y_{i_l}, Y_{i_u}]$

$R_{2c} : [R_{2lc}, R_{2uc}]$: IF x is $[X_{(i+1)_l}, X_{(i+1)_u}]$ THEN Δu_c is $[Y_{(i+1)_l}, Y_{(i+1)_u}]$

C. Inference mechanism

Figure 3 represents the inferred output FSs along with their MFs using LP inference, whose mathematical description is given in Equations (10)-(13).

$$\mu_{Y'_{i_l}} = \begin{cases} 0 & \text{if } L_{y_{i-1}} \le \Delta u_c \le (L_{y_{i-1}} + P_{y_{i-1}}) \\ \frac{\mu_{X_{i_l}}(\Delta u_c - L_{y_{i-1}} - P_{y_{i-1}})}{L_{y_i} - L_{y_{i-1}} - P_{y_{i-1}}} & \\ & \text{if } (L_{y_{i-1}} + P_{y_{i-1}}) \le \Delta u_c \le L_{y_i} \\ \frac{\mu_{X_{i_l}}(-\Delta u_c + L_{y_{i+1}} - P_{y_i})}{L_{y_{i+1}} - L_{y_i} - P_{y_i}} & \\ & \text{if } L_{y_i} \le \Delta u_c \le (L_{y_{i+1}} - P_{y_i}) \\ 0 & \text{if } (L_{y_{i+1}} - P_{y_i}) \le \Delta u_c \le L_{y_{i+1}} \end{cases} \quad (10)$$

$$\mu_{Y'_{i_u}} = \begin{cases} \frac{\mu_{X_{i_u}}(\Delta u_c - L_{y_{i-1}})}{L_{y_i} - L_{y_{i-1}}} & \text{if } L_{y_{i-1}} \le \Delta u_c \le L_{y_i} \\ \frac{\mu_{X_{i_u}}(-\Delta u_c + L_{y_{i+1}})}{L_{y_{i+1}} - L_{y_i}} & \text{if } L_{y_i} \le \Delta u_c \le L_{y_{i+1}} \end{cases} \quad (11)$$

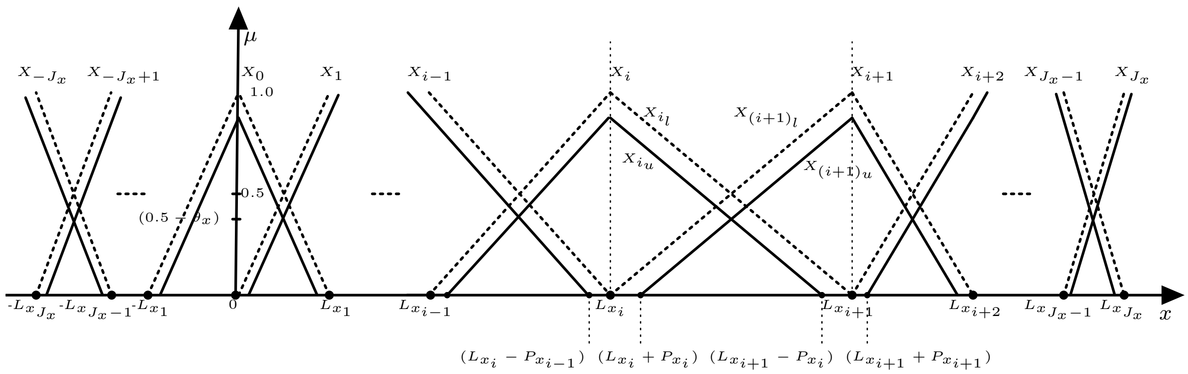

Fig. 1: Input IT2 FSs

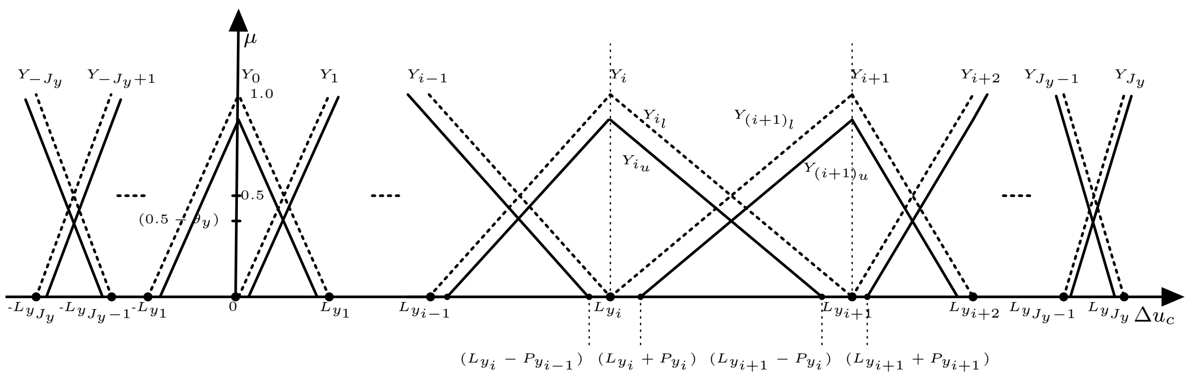

Fig. 2: Output IT2 FSs

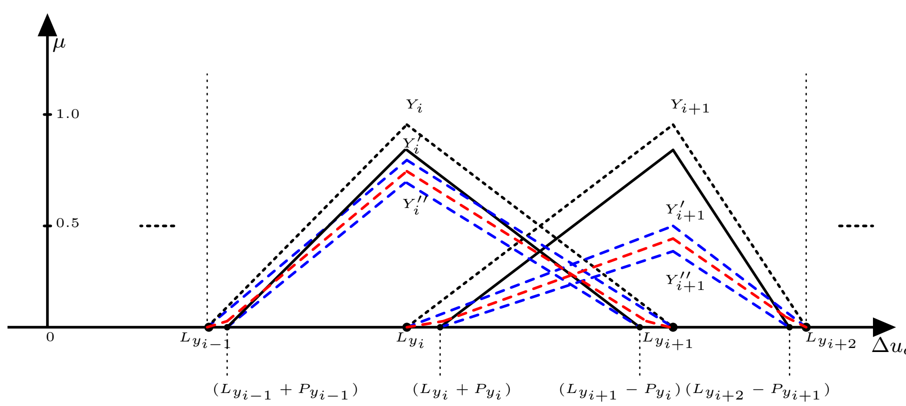

Fig. 3: Inferred output IT2 FSs

$$\mu_{Y'_{(i+1)_u}} = \begin{cases} \frac{\mu_{X_{(i+1)_u}}(\Delta u_c - L_{y_i})}{L_{y_{i+1}} - L_{y_i}} & \text{if } L_{y_i} \le \Delta u_c \le L_{y_{i+1}} \\ \frac{\mu_{X_{(i+1)_u}}(-\Delta u_c + L_{y_{i+2}})}{L_{y_{i+2}} - L_{y_{i+1}}} & \text{if} L_{y_{i+1}} \le \Delta u_c \le L_{y_{i+2}} \end{cases} \tag{12}$$

$$\mu_{Y'_{(i+1)_l}} = \begin{cases} 0 & \text{if } L_{y_i} \le \Delta u_c \le (L_{y_i} + P_{y_i}) \\ \frac{\mu_{X_{(i+1)_l}}(\Delta u_c - L_{y_i} - P_{y_i})}{L_{y_{i+1}} - L_{y_i} - P_{y_i}} & \\ & \text{if } (L_{y_i} + P_{y_i}) \le \Delta u_c \le L_{y_{i+1}} \\ \frac{\mu_{X_{(i+1)_l}}(-\Delta u_c + L_{y_{i+2}} - P_{y_{i+1}})}{L_{y_{i+2}} - L_{y_{i+1}} - P_{y_{i+1}}} & \\ & \text{if } L_{y_{i+1}} \le \Delta u_c \le (L_{y_{i+2}} - P_{y_{i+1}}) \\ 0 & \text{if } (L_{y_{i+2}} - P_{y_{i+1}}) \le \Delta u_c \le L_{y_{i+2}} \end{cases} \tag{13}$$

We have used an input space of 1D as shown in Fig. 4 to model the controller. This space is partitioned into different regions, and each region is partitioned into three zones. The Δu_c of the newly obtained controller in each zone of each region is derived.

D. Output processing

It includes type reduction followed by defuzzification.
(1) Type reduction: It creates a T1 FS from an IT2 FS. Numerous TR algorithms have been documented in the literature.

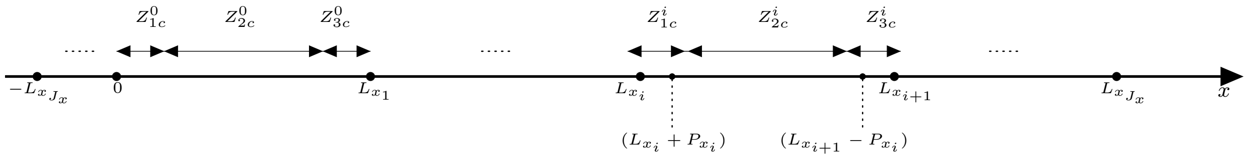

Fig. 4: Partitioned 1D input space

(2) Defuzzification: A defuzzifier converts a fuzzy value into a crisp value. This work uses the NT defuzzification method. **NT defuzzifier:** Mendel and Liu [5] used the NT defuzzifier to make it easier to calculate the defuzzified outcome of an IT2 fuzzy logic system. It is indeed a direct TR algorithm that obtains the defuzzified output by averaging the lower bounds $\underline{\mu}_{\tilde{A}}$ and higher bounds $\overline{\mu}_{\tilde{A}}$. The defuzzified value of a given IT2 FS $\tilde{A}$ with specified FoU in [a,b] using NT method is provided in (14).

$$\Delta u_c = \frac{\int_a^b (\underline{\mu}_{\tilde{A}} + \overline{\mu}_{\tilde{A}})\Delta u_c d\Delta u_c}{\int_a^b (\underline{\mu}_{\tilde{A}} + \overline{\mu}_{\tilde{A}}) d\Delta u_c} = \frac{\int_a^b \mu_{\tilde{A}-AVG}\Delta u_c d\Delta u_c}{\int_a^b \mu_{\tilde{A}-AVG} d\Delta u_c} \tag{14}$$

III. MATHEMATICAL MODELS

We derive the Δu_c of developed controller by referring to Fig. 3 as

$$\Delta u_c = \frac{C_{Y_i''}A_{Y_i''} + C_{Y_{i+1}''}A_{Y_{i+1}''}}{A_{Y_i''} + A_{Y_{i+1}''}} \tag{15}$$

where $C_{Y_i''}$ and $C_{Y_{(i+1)}''}$ are the centroids and $A_{Y_i''}$ and $A_{Y_{(i+1)}''}$ are areas related to FSs Y_i'' and $Y_{(i+1)}''$ whose MFs, indicated by red dotted lines as illustrated in Fig. 3, are expressed in (16) and (17). The areas and centroids in (15) are computed by using (16) and (17) in (18)-(21).

$$\mu_{Y_i''} = \begin{cases} \frac{\mu_{X_{i_u}}(\Delta u_c - L_{y_{i-1}})}{2(L_{y_i} - L_{y_{i-1}})} \\ \quad \text{if } \; L_{y_{i-1}} \le \Delta u_c \le (L_{y_{i-1}} + P_{y_{i-1}}) \\ \frac{\mu_{X_{i_l}}[\Delta u_c - (L_{y_{i-1}} + P_{y_{i-1}})]}{2(L_{y_i} - L_{y_{i-1}} - P_{y_{i-1}})} + \frac{\mu_{X_{i_u}}[\Delta u_c - L_{y_{i-1}}]}{2(L_{y_i} - L_{y_{i-1}})} \\ \quad \text{if } \; (L_{y_{i-1}} + P_{y_{i-1}}) \le \Delta u_c \le L_{y_i} \\ \frac{\mu_{X_{i_l}}[-\Delta u_c + (L_{y_{i+1}} - P_{y_i})]}{2(L_{y_{i+1}} - L_{y_i} - P_{y_i})} + \frac{\mu_{X_{i_u}}[-\Delta u_c + L_{y_{i+1}}]}{2(L_{y_{i+1}} - L_{y_i})} \\ \quad \text{if } \; L_{y_i} \le \Delta u_c \le (L_{y_{i+1}} - P_{y_i}) \\ \frac{\mu_{X_{i_u}}(-\Delta u_c + L_{y_{i+1}})}{2(L_{y_{i+1}} - L_{y_i})} \\ \quad \text{if } \; (L_{y_{i+1}} - P_{y_i}) \le \Delta u_c \le L_{y_{i+1}} \end{cases} \tag{16}$$

$$\mu_{Y_{(i+1)}''} = \begin{cases} \frac{\mu_{X_{(i+1)_u}}(\Delta u_c - L_{y_i})}{2(L_{y_{i+1}} - L_{y_i})} \\ \quad \text{if } \; L_{y_i} \le \Delta u_c \le (L_{y_i} + P_{y_i}) \\ \frac{\mu_{X_{(i+1)_l}}[\Delta u_c - (L_{y_i} + P_{y_i})]}{2(L_{y_{i+1}} - L_{y_i} - P_{y_i})} + \frac{\mu_{X_{(i+1)_u}}[\Delta u_c - L_{y_i}]}{2(L_{y_{i+1}} - L_{y_i})} \\ \quad \text{if } \; (L_{y_i} + P_{y_i}) \le \Delta u_c \le L_{y_{i+1}} \\ \frac{\mu_{X_{(i+1)_l}}[-\Delta u_c + (L_{y_{i+2}} - P_{y_{i+1}})]}{2(L_{y_{i+2}} - L_{y_{i+1}} - P_{y_{i+1}})} + \frac{\mu_{X_{(i+1)_u}}[-\Delta u_c + L_{y_{i+2}}]}{2(L_{y_{i+2}} - L_{y_{i+1}})} \\ \quad \text{if } \; L_{y_{i+1}} \le \Delta u_c \le (L_{y_{i+2}} - P_{y_{i+1}}) \\ \frac{\mu_{X_{(i+1)_u}}(-\Delta u_c + L_{y_{i+2}})}{2(L_{y_{i+2}} - L_{y_{i+1}})} \\ \quad \text{if } \; (L_{y_{i+2}} - P_{y_{i+1}}) \le \Delta u_c \le L_{y_{i+2}} \end{cases} \tag{17}$$

$$C_{Y_i''} = \frac{\begin{array}{c}(L_{y_{i-1}} + L_{y_i} + L_{y_{i+1}} + P_{y_{i-1}} - P_{y_i})(L_{y_{i-1}} \\ -L_{y_{i+1}} + P_{y_{i-1}} + P_{y_i})\mu_{X_{i_l}} + (L_{y_{i-1}} - L_{y_{i+1}}) \\ (L_{y_{i-1}} + L_{y_i} + L_{y_{i+1}})\mu_{X_{i_u}}\end{array}}{\begin{array}{c}3[(P_{y_{i-1}} + P_{y_i})\mu_{X_{i_l}} + (L_{y_{i-1}} - L_{y_{i+1}}) \\ (\mu_{X_{i_l}} + \mu_{X_{i_u}})]\end{array}} \tag{18}$$

$$C_{Y_{i+1}''} = \frac{\begin{array}{c}(L_{y_i} + L_{y_{i+1}} + L_{y_{i+2}} + P_{y_i} - P_{y_{i+1}})(L_{y_i} - \\ L_{y_{i+2}} + P_{y_i} + P_{y_{i+1}})\mu_{X_{(i+1)_l}} + (L_{y_i} - L_{y_{i+2}}) \\ (L_{y_i} + L_{y_{i+1}} + L_{y_{i+2}})\mu_{X_{(i+1)_u}}\end{array}}{\begin{array}{c}3[(P_{y_i} + P_{y_{i+1}})\mu_{X_{(i+1)_l}} + (L_{y_i} - L_{y_{i+2}}) \\ (\mu_{X_{(i+1)_l}} + \mu_{X_{(i+1)_u}})]\end{array}} \tag{19}$$

$$A_{Y_i''} = -\frac{\begin{array}{c}[(P_{y_{i-1}} + P_{y_i})\mu_{X_{i_l}} + (L_{y_{i-1}} - L_{y_{i+1}}) \\ (\mu_{X_{i_l}} + \mu_{X_{i_u}})]\end{array}}{4} \tag{20}$$

$$A_{Y_{i+1}''} = -\frac{\begin{array}{c}[(P_{y_i} + P_{y_{i+1}})\mu_{X_{(i+1)_l}} + (L_{y_i} - L_{y_{i+2}}) \\ (\mu_{X_{(i+1)_l}} + \mu_{X_{(i+1)_u}})]\end{array}}{4} \tag{21}$$

Table III provides the resulting expression of Δu_c for each zone of middle regions of Fig. 4.
By substituting c with P, I, or D, x with Δe_s, e_s, or $\Delta^2 e_s$, and y with Δu_P, Δu_I, or Δu_D, respectively, the IT2 FP, FI, or FD controller models can be generated.

A. PROPERTIES

By randomly selecting the values of $J_x = J_y = 3$, $\theta_x = \theta_y = 0.3$, $L_{x_1} = L_{y_1} = 2$, $L_{x_2} = L_{y_2} = 4$ and $L_{x_3} = L_{y_3} = 6$ for controllers with UD FSs, and $L_{x_1} = L_{y_1} = 3$, $L_{x_2} = L_{y_2} = 5$ and $L_{x_3} = L_{y_3} = 6$ for controllers with NUD FSs, the input-output relations of the newly developed controller are illustrated in Fig. 5

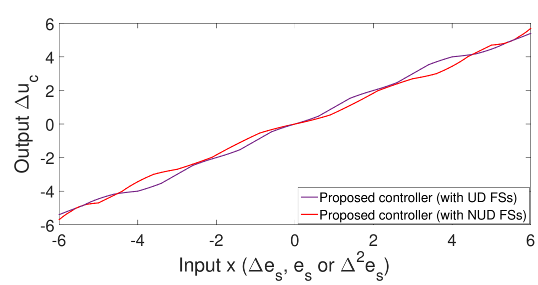

Fig. 5: Input-output relation

- The relation between input-output variables around the point of origin is symmetric, as seen in Fig. 5. Furthermore, it is evident that the structures of the controllers

TABLE III: Mathematical models of the controller when two full output FSs in the middle regions are fired

Zone	Δu_c
Z^i_{1c}, Z^i_{3c}	$\frac{L_{x_{i+a}}(L_{y_{i-b}} - L_{y_{i+2-b}})(L_{y_{i-b}} + L_{y_{i+1-b}} + L_{y_{i+2-b}}) - L_{x_{i+1-a}}[2L^2_{y_{i-1+b}} - 2L^2_{y_{i+1+b}} + 2L_{y_{i-1+b}}(L_{y_{i+b}} + P_{y_{i-1+b}}) + L_{y_{i+b}}(-2L_{y_{i+1+b}} + P_{y_{i-1+b}} + P_{y_{i+b}}) + 2L_{y_{i+1+b}}P_{y_{i+b}} + P^2_{y_{i-1+b}} - P^2_{y_{i+b}}] \pm P_{x_i}(L_{y_{i-1+b}} + L_{y_{i+b}} + L_{y_{i+1+b}} + P_{y_{i-1+b}} - P_{y_{i+b}})(L_{y_{i-1+b}} - L_{y_{i+1+b}} + P_{y_{i-1+b}} + P_{y_{i+b}}) + [2L^2_{y_{i-1+b}} - L^2_{y_{i-b}} - 2L^2_{y_{i+1+b}} + L^2_{y_{i+2-b}} + (2L_{y_{i-1+b}} + L_{y_{i+b}})P_{y_{i-1+b}} + (L_{y_{i+b}} + 2L_{y_{i+1+b}})P_{y_{i+b}} \pm (2L_{y_{i-1+b1}}L_{y_{i+b1}} - 3L_{y_i}L_{y_{i+1}} + L_{y_{i+1-b1}}L_{y_{i+2-b1}}) + (P^2_{y_{i-1+b}} - P^2_{y_{i+b}})]x}{3[L_{x_{i+a}}(L_{y_{i-b}} - L_{y_{i+2-b}}) - L_{x_{i+1-a}}(2L_{y_{i-1+b}} - 2L_{y_{i+1+b}} + P_{y_{i-1+b}} + P_{y_{i+b}}) \pm P_{x_i}(L_{y_{i-1+b}} - L_{y_{i+1+b}} + P_{y_{i-1+b}} + P_{y_{i+b}}) + (2L_{y_{i-1+b}} - L_{y_{i-b}} - 2L_{y_{i+1+b}} + L_{y_{i+2-b}} + P_{y_{i-1+b}} + P_{y_{i+b}})x]}$
Z^i_{2c}	$\frac{L_{x_{i+1}}[2L^2_{y_{i-1}} - 2L^2_{y_{i+1}} + 2L_{y_{i-1}}(L_{y_i} + P_{y_{i-1}}) + L_{y_i}(-2L_{y_{i+1}} + P_{y_{i-1}} + P_{y_i}) + 2L_{x_{i+1}}P_{y_i} + P^2_{y_{i-1}} - P^2_{y_i}] - P_{x_i}[L^2_{y_{i-1}} + L^2_{y_i} - L^2_{y_{i+1}} - L^2_{y_{i+2}} + L_{y_{i-1}}(L_{y_i} + 2P_{y_{i-1}}) + L_{y_i}(P_{y_{i-1}} + 3P_{y_i}) + L_{y_{i+1}}(3P_{y_i} + P_{y_{i+1}}) - L_{y_{i+2}}(L_{y_{i+1}} - 2P_{y_{i+1}}) + P^2_{y_{i-1}} - P^2_{y_{i+1}}] - L_{x_i}[2L^2_{y_i} - 2L^2_{y_{i+2}} + 2L_{y_i}(L_{y_{i+2}} + P_{y_i}) + L_{y_{i+1}}(-2L_{y_{i+2}} + P_{y_i} + P_{y_{i+1}}) + 2L_{y_{i+2}}P_{y_{i+1}} + P^2_{y_i} - P^2_{y_{i+1}}] - [2L^2_{y_{i-1}} - 2L^2_{y_i} - 2L^2_{y_{i+1}} + 2L^2_{y_{i+2}} + 2L_{y_{i-1}}(L_{y_i} + P_{y_{i-1}}) + L_{y_i}(-4L_{y_{i+1}} + P_{y_{i-1}} - P_{y_i}) + L_{y_{i+1}}(2L_{y_{i+2}} + P_{y_i} - P_{y_{i+1}}) - 2L_{y_{i+2}}P_{y_{i+1}} + P^2_{y_{i-1}} - 2P^2_{y_i} + P^2_{y_{i+1}}]x}{3[L_{x_{i+1}}(2L_{y_{i-1}} - 2L_{y_{i+1}} + P_{y_{i-1}} + P_{y_i}) - L_{x_i}(2L_{y_i} - 2L_{y_{i+2}} + P_{y_i} + P_{y_{i+1}}) - P_{x_i}(L_{y_{i-1}} + L_{y_i} - L_{y_{i+1}} - L_{y_{i+2}} + P_{y_{i-1}} + 2P_{y_i} + P_{y_{i+1}}) - (2L_{y_{i-1}} - 2L_{y_i} - 2L_{y_{i+1}} + 2L_{y_{i+2}} + P_{y_{i-1}} - P_{y_{i+1}})x]}$

Note: $a = 0$, $b = 0$, $b1 = 0$ and upper sign for Z^i_{1c}
$a = 1$, $b = 1$, $b1 = 2$ and lower sign for Z^i_{3c}.

are nonlinear in other zones and linear near the point of origin.

- The developed controller is a variable-gain and variable-structure controller. Additionally, it is nonlinear and free from a plant model.
- The magnitude of Δu_c increases monotonically as the magnitude of the input increases, and it is zero when the input is zero.

Genetic algorithm [1] optimization method is used for tuning the controller parameters by optimizing the cost function given in the following equation:

$$J_c = T \sum_{k=0}^{N-1} [e^2(k) + u^2(k)] \quad (22)$$

where $N = T_f/T$ and the notations $e(k)$, $u(k)$, T, and T_f denote the error signal, control signal, sampling time, and final time of interest, respectively.

IV. SIMULATION STUDY

The nonlinear system's dynamics from [8] given in (23)

$$\dot{y}(t) = c_1 y(t) + \sin^2(\sqrt{|c_2 y(t)|}) + u(t) \quad (23)$$

is examined here to verify that the newly developed controller is valid and applicable. In (23), $u(t)$ is the input and $y(t)$ is the output of the plant. The chosen values for $c_1 = 1$, $c_2 = 1$, $T = 0.001\ s$ and $T_f = 1.5\ s$. Here, the reference is a unit step function. $K^d_P = 100$, $K^d_I = 300$, and $K^d_D = 20$ are the optimal parameters of linear PID controller. The values of the optimal parameters of the newly developed controller are provided in Table IV.

TABLE IV: Parameters of controller

Parameter	UD	NUD	Parameter	UD	NUD
K^d_P	1.01	10	$L_{\Delta u_{P2}}$	$\frac{2L_{\Delta u_{P3}}}{3}$	0.8
K^d_I	0.9	1.01	$L_{\Delta u_{P3}}$	1.77	2.7
K^d_D	0.003	7	$L_{\Delta u_{I1}}$	$\frac{L_{\Delta u_{I3}}}{3}$	0.4
K_0	10	14.75	$L_{\Delta u_{I2}}$	$\frac{2L_{\Delta u_{I3}}}{3}$	0.8
L_{e_1}	$\frac{L_{e_3}}{3}$	0.1	$L_{\Delta u_{I3}}$	0.153	2.7
L_{e_2}	$\frac{2L_{e_3}}{3}$	0.3	$L_{\Delta u_{D1}}$	$\frac{L_{\Delta u_{D3}}}{3}$	0.4
L_{e_3}	0.1167	1	$L_{\Delta u_{D2}}$	$\frac{2L_{\Delta u_{D3}}}{3}$	0.8
$L_{\Delta e_1}$	$\frac{L_{\Delta e_3}}{3}$	0.1	$L_{\Delta u_{D3}}$	0.153	0.27
$L_{\Delta e_2}$	$\frac{2L_{\Delta e_3}}{3}$	0.3	θ_e	0.36	0.12
$L_{\Delta e_3}$	0.297	1	$\theta_{\Delta e}$	0.01	0.12
$L_{\Delta^2 e_1}$	$\frac{L_{\Delta^2 e_3}}{3}$	0.1	$\theta_{\Delta^2 e}$	0.01	0.12
$L_{\Delta^2 e_2}$	$\frac{2L_{\Delta^2 e_3}}{3}$	0.3	$\theta_{\Delta u_P}$	0.42	0.32
$L_{\Delta^2 e_3}$	0.297	1	$\theta_{\Delta u_I}$	0.01	0.32
$L_{\Delta u_{P1}}$	$\frac{L_{\Delta u_{P3}}}{3}$	0.4	$\theta_{\Delta u_D}$	0.01	0.32

Figures 6(a) and 6(b), respectively, display the responses and the accompanying control signals of the developed IT2 FPID controller with UD and NUD FSs.

To test the disturbance rejection ability, we introduced a disturbance (a step disturbance of magnitude 0.2) at the plant output side for $t \geq 0.5\ s$, and the robustness property of the developed controllers is tested by increasing the parameters c_1 and c_2 by 50 %. Figs. 6((c)-(f)) display the responses and accompanying control signals of linear PID, FPID [8], IT2 FPID [10], and the developed IT2 FPID controller with UD and NUD FSs.

The effectiveness of the proposed IT2 FPID controller is demonstrated by comparing the performances of the plant with the linear PID controller, FPID [8] controller, IT2 FPID [10] controller, and the proposed IT2 FPID controller with UD and NUD FSs in terms of rise time (t_r), settling time (t_s), maximum peak (M_p), steady state error (e_{ss}), control energy ($E_u = T\sum_{k=0}^{N-1}[u^2(k)]$), and J_c, provided in Table V.

TABLE V: Time-domain performance data

Controller	$t_r(s)$	$t_s(s)$	$M_P(\%)$	e_{ss}	E_u	J_c
Linear PID	0.02	0.029	4.1	0	63.07	63.07
Fuzzy PID [8]	0.022	0.0263	1.83	0	48.88	48.89
IT2 fuzzy PID [10]	0.018	0.032	0	0	42.25	45.39
Proposed controller						
(with UD)	0.06	0.09	0	0	**16.86**	**16.89**
(with NUD)	**0.0112**	**0.017**	0.1	0	84.82	84.82

Observations:

- The IT2 FPID [10] and the controller with UD FSs produce no M_P.
- The proposed IT2 FPID controller with NUD FSs performs the best in terms of t_r and t_s, and the controller with UD FSs in terms of E_u and J_c.

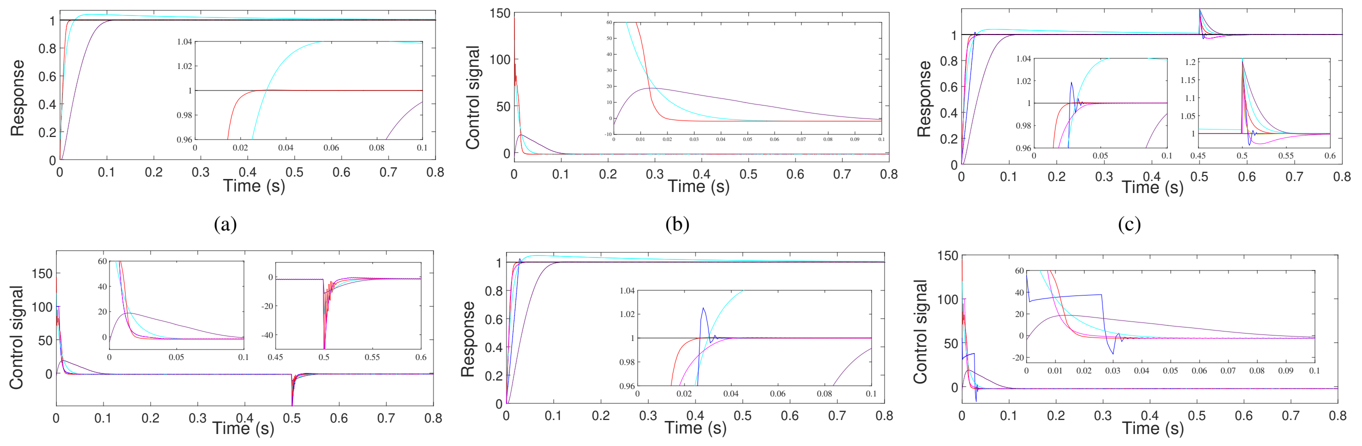

(a) (b) (c) (d) (e) (f)

Fig. 6: (a) Step response (b) Control signal (c) Step response with disturbance (d) Control signal with disturbance (e) Step response with parameter uncertainty (f) Control signal with parameter uncertainty
Note: —— Linear PID, —— Fuzzy PID [8], —— IT2 fuzzy PID [10], —— Proposed controller (with UD FSs), —— Proposed controller (with NUD FSs)

- In general, the controller with NUD FSs performs better than the controller with UD FSs, as shown in Table V.
- The plant responses due to the proposed controller do not change significantly in the presence of disturbance and plant parameter uncertainty.

V. CONCLUSIONS

This work presented the analytical structures of a general IT2 FPID controller. NUD triangular FSs are used for input and output variables. Based on the NT defuzzification method, the analytical structures of the developed controller are obtained and carefully examined for their properties. Finally, the robustness property of the proposed controller is demonstrated through simulation studies by considering output disturbance and plant parameter uncertainty. The primary benefit of the proposed 1D input space approach is that it allows for independent tuning of proportional, integral, and derivative channels of the PID controller as its nonlinear proportional, integral, and derivative gains are uncoupled. To demonstrate the non-uniform characteristics of the FSs, the locations and widths were selected randomly. A potential direction for future research is the development of a systematic technique for determining the locations and widths of non-uniform triangular FSs.

REFERENCES

[1] D.E. Goldberg, "Genetic algorithms in search, optimization and machine learning," *Addison-Wesley Publishing Company*, Inc, 1989.

[2] F.L. Lewis and K. Liu, "Towards a paradigm for fuzzy logic control," *Automatica*, vol. 32, no. 2, pp. 167–181, 1996.

[3] X. Du and H. Ying, "Derivation and analysis of the analytical structures of the interval type-2 fuzzy PI and PD controllers," *IEEE Trans. Fuzzy Syst.*, vol. 18, no. 4, pp. 802-814, 2010.

[4] M. Nie and W. W. Tan, "Analytical structure and characteristics of symmetric Karnik–Mendel type-reduced interval type-2 fuzzy PI and PD controllers," *IEEE Trans. Fuzzy Syst.*, vol. 20, no. 3, pp. 416–430, 2012.

[5] J.M. Mendel and X. Liu, "Simplified interval type-2 fuzzy logic systems," *IEEE Trans. Fuzzy Syst.*, vol. 21, no. 6, pp. 1056–1069, 2013.

[6] A.M. El-Nagar and M. El-Bardini, "Derivation and stability analysis of the analytical structures of the interval type-2 fuzzy PID controller," *App. Soft Comput.*, vol. 24, pp. 704-716, 2014.

[7] A. Kumar and V. Kumar, "A novel interval type-2 fractional order fuzzy PID controller: Design, performance evaluation, and its optimal time domain tuning," *ISA Trans.*, vol. 68, pp. 251-275, 2017.

[8] D. Sain and B.M. Mohan, "Modelling of a nonlinear fuzzy three-input PID controller and its simulation and experimental realization," *IETE Technical Review*, vol. 38, no. 5, pp. 479–498, 2020.

[9] D. Sain, M. Praharaj, and B. M. Mohan, "A simple modelling strategy for integer order and fractional order interval type-2 fuzzy PID controllers with their simulation and real-time implementation," *Expert Syst. Appl.*, vol. 202, no. 1, pp. 117196, 2022.

[10] M. Praharaj, D. Sain, and B. M. Mohan, "Development, experimental validation, and comparison of interval type-2 Mamdani fuzzy PID controllers with different footprints of uncertainty," *Inf. Sci.*, vol. 601, no. 3, pp. 374–402, 2022.

[11] Y. Wang, Z. Wang, L. Zou, Q. Ge, and H. Dong, "Observer-based fuzzy PID control for nonlinear systems with degraded measurements: dealing with randomly perturbed sampling periods," *IEEE Trans. Fuzzy Syst.*, vol. 32, no. 12, pp. 6848-6862, 2024.

[12] D. Sain and T. H. Lee, "Novel mathematical modeling of IT2 Takagi–Sugeno fuzzy PID controllers with triangular FoUs and their application: A MagLev case study," *Appl. Soft Comput.*, vol. 191, pp. 114663, 2026.